Thermal Science and Engineering Progress 4 (2017) 150–159

Contents lists available at ScienceDirect

Thermal Science and Engineering Progress

journal homepage: www.elsevier.com/locate/tsep

Boundary layer flow heat and mass transfer study of Sakiadis flow of viscoelastic nanofluids using hybrid neural network-particle swarm optimization (HNNPSO)

Aminreza Noghrehabadi [a], Reza Mirzaei [a], Mohammad Ghalambaz [b,*], Ali Chamkha [c,d], Afshin Ghanbarzadeh [a]

[a] Department of Mechanical Engineering, Shahid Chamran University of Ahvaz, Ahvaz, Iran
[b] Department of Mechanical Engineering, Dezful Branch, Islamic Azad University, Dezful, Iran
[c] Mechanical Engineering Department, Prince Mohammad Bin Fahd University (PMU), Al-Khobar 31952, Saudi Arabia
[d] Prince Sultan Endowment for Energy and Environment, Prince Mohammad Bin Fahd University, Al-Khobar 31952, Saudi Arabia

ARTICLE INFO

Article history:
Received 23 May 2017
Received in revised form 9 August 2017
Accepted 9 September 2017

Keywords:
Viscoelastic nanofluid
Similarity equations
Intelligent methods
Optimization algorithm
Neural network

ABSTRACT

Viscoelastic nanofluids equations are mainly ill-posed at the system boundaries, and hence, achieving a numerical solution faces serious challenges. In addition, the presence of very fine nanoparticles (with the mean size of 100 nm and lower) in the fluid leads to new phenomena of heat and particle transfer, which highly increases the non-linearity and complexity of the behavior of the resulting viscoelastic nanofluids. Thus, new analytical or semi-analytical methods are highly demanded to deal with flow and heat transfer of viscoelastic nanofluids. In this study, by a new idea using intelligent optimization methods, a new and unique method is presented to solve the differential equations governing flow and heat transfer of viscoelastic nanofluids. Using intelligent optimization, it is attempted to move towards an optimum solution by changing a trial solution that satisfies both the governing equations and the boundary conditions as well. The results indicate the accuracy and simplicity of the method.

1. Introduction

Given the broad range of non-Newtonian fluids applications in various branches of engineering sciences including oil, roller and plastic extrusion operations, many researchers' attention has been drawn to the flow and heat transfer of these fluids [1]. Moreover, the presence of nanoparticles in the fluid could result in new properties to the base fluid. For example, the presence of ZnO or TiO_2 nanoparticles in the base fluid induces anti-bacterial properties [2,3]. The presence of nanoparticles in the base fluid can directly absorb the solar heat in the solar collectors [4,5]. In the meantime, since heat transfer in nanofluids is higher than conventional fluids, the enhancement of heat transfer of non-Newtonian nanofluids and viscoelastic fluids in particular is of interest for many researchers.

A Newtonian fluid is a substance in which the shear stress is only a linear function of the shear rate. Accordingly, a non-Newtonian fluid can be defined simply as a fluid without a Newtonian behavior. One of the non-Newtonian fluids is the viscoelastic fluid, which has both viscous and elastic properties simultaneously. Viscoelastic fluids play a crucial role in chemistry, biochemistry and food industry. Also, viscoelastic fluid flow applications are transmission of the oil based materials in the oil and petrochemical industries, food production industries, manufacturing of chemicals and detergents, polymer injection, cooling of turbine blades and so on [1,6].

Many fluids' behavior can be described by non-linear differential equations. There are several numerical and analytical approaches for solving non-linear differential equations. However, the solution of many high-order ill-posed differential equations is still a major challenge. Unfortunately, for many non-linear differential equations, finding an exact analytical solution is not easy and is often impossible due to nonlinearity of the equations. In this case, an estimate of the solution can be obtained using a series semi-analytical method, Homotopy method and/or numerical methods such as Euler, Runge-Kutta, finite difference, finite volume, etc. Depending on the differential equations and their

* Corresponding author.
E-mail addresses: noghrehabadi@scu.ac.ir (A. Noghrehabadi), reza_mirzaei1989@yahoo.com (R. Mirzaei), m.ghalambaz@iaud.ac.ir (M. Ghalambaz), achamkha@pmu.edu.sa (A. Chamkha), ghanbarzadeh.a@scu.ac.ir (A. Ghanbarzadeh).

https://doi.org/10.1016/j.tsep.2017.09.003
2451-9049/

behavior, some methods are more appropriate than others and some methods may not reach the correct solution.

The governing equations of the viscoelastic nanofluids and heat transfer are inherently nonlinear and mainly ill-posed at the system boundaries. Hence, obtaining a numerical solution for these fluids faces serious challenges. In these equations, the term related to the highest derivative in the differential equation is zero at the boundary. In this case, most of the conventional numerical or analytical methods fail to obtain a solution for the problem. Thus, developing new solution methods, dealing with the governing equations arising from the viscoelastic nanofluids is highly demanded.

There are several analytical methods, which can deal with the differential equations arising from the viscoelastic flows, such as perturbation method [7], Homotopy Analysis Method (HAM) [8] and Adomian Decomposition Method (ADM) [9].

The main disadvantage of the perturbation method is that the method is inherently based on large and small parameters in question known as perturbation values and it is impossible that all nonlinear problems have such perturbation values, and the method is applied for cases that the equation is weakly nonlinear. The convergence range of the power series obtained by the Adomian decomposition method is low, and hence, it is unable to deal with asymptotic boundary value problems. The main disadvantage of the Homotopy analysis method is that the method is dependent on a convergence-parameter control (h). If one selects an incorrect parameter h, the solution may be divergent. In addition, to achieve an appropriate solution, a large number of analytical sentences is also needed.

In recent years, a number of researchers have investigated viscoelastic fluids equations in boundary layers. Sadeghi and Sharifi [10] proposed a similarity solution to the boundary layer equations for a viscoelastic fluid of second order flowing over a moving plate. Cortell [11] has investigated the viscoelastic fluids' flow and heat transfer over a moving semi-infinite horizontal plate. Cortell identified an important behavior for viscoelastic flows, which shows that a change in the behavior of the fluid occurs at a critical Weissenberg number (approximately equal to one). Munawar et al. [12] published a comment on the study of Cortell [11] and demonstrated that the governing differential equations for flow of viscoelastic flows derived Sadeghi and Sharifi [10] that has also been used in Cortell [11] study needs some corrections. Then they [12] provided a new solution for the corrected form of the governing equation using the Homotopy Analysis Method (HAM). The results reported by Munawar et al. [12] do not confirm the presence of a critical Weissenberg number about unity. Tonekaboni et al. [13] have investigated the boundary layer flow of a second-order viscoelastic fluid. They utilized the fourth-order predictive-corrective finite-difference method to solve the governing equations. They reported that by increasing the fluid elasticity, the wall shear stress is increased for a stagnation-point flow and is decreased for the Blasius and Sakiadis flows. Ramesh et al. [14] have studied the mixed convection boundary layer flow over an inclined stretching surface immersed in an incompressible viscoelastic fluid, and found that velocity decreases as the value of angle of inclination increases. Duwairi et al. [15] examined the viscoelsatic boundary layer flow and the heat transfer near a vertical isothermal impermeable surface. They have shown that the coefficients of friction and heat transfer enhance for higher viscoelsatic parameters.

The term nanofluid was introduced by Choi [16] and is said to be a new type of fluid in which metal or non-metal particles smaller than 100 nm in size are in suspended in a base fluid. The increase in the resulting mechanical properties such as the thermal conductivity coefficient, fluid viscosity and the heat transfer coefficient is unique a property of these fluids compared to base fluids [17]. Buongiorno [18] has investigated different heat transfer mechanisms of nanofluids displacement by performing different experiments. He concluded that high heat transfer increase in nanofluids is mainly caused by Brownian motion of particles and thermophoresis effect. It is noteworthy that thermophoresis effect is implied to the force applied opposed to temperature gradient on particles existing in solution. There are excellent studies on different engineering aspects of nanofluids such as boundary layer flows [19,20] natural convection [21–23], mixed convection flows [24–27], heat transfer in porous media [28], Newtonian and non-Newtonian nanofluids [29–32], heat transfer with radiation [33–35] and heat transfer with phase change [36]. The magnetic nanofluids are a new type of nanofluids flow in which the flow and heat transfer is under the significant influence of a magnetic field. The effect of a magnetic field on the flow and heat transfer of nanofluids has been studied in the literature [37,38]. There are also types of nanofluids containing magnetic nanoparticles [39–41].

Sheu et al. [42] have investigated convective heat transfer in boundary layer flows of viscoelastic nanofluids. They modeled the viscoelastic nanofluids rheological behavior by using Oldroyd-B model and examined natural convection heat transfer. Yang et al. [43] have experimentally measured the viscosity and the thermal conductivity of a viscoelastic-fluid-based nanofluid (a viscoelastic fluid as the base fluid and copper nanoparticles). Goyal et al. [44] have theoretically studied the flow and heat transfer of a second-order viscoelastic nanofluid over a stretching sheet. They have solved the governing equations of a viscoelastic nanofluid over a stretching sheet with a heat source/sink, under the action of a uniform magnetic field, orientated normally to the plate using the finite element method.

Artificial neural networks are systems and new computational methods for machine learning and its application to predict the output responses of complex systems. The main idea of these networks is inspired by biological nervous system performance. Artificial neural networks have shown very high performance in estimation and approximation of functions [45].

Optimization is a mathematical tool that is used to find the solution of many questions on how to solve various problems. To this end, researchers and engineers in recent years have simulated methods of artificial intelligence and computational method of these methods to the logic of organisms' life by studying the lifestyle of some of organisms and their logics. The birds' lifestyle that is the pattern of particle swarm optimization [46] and also bees' logic of life that is the pattern of a bee colony optimization [47] are two examples of artificial intelligence optimization methods.

Recently, new synthetic methods have been developed by which differential equations governing engineering problems can be solved. Lee and Kang [48] used parallel processing computers to obtain an approximate solution to the first-order differential equations. In another method, Meade and Fernandez [49] and Lagaris et al. [50] using a neural network have solved ordinary and partial differential equations. Malek and Shekari Beidokhti [51] used a combination of neural network and intelligent optimization methods for solving higher-order differential equations. They solved higher-order differential equations by using a neural network and Nelder-Mead optimization.

In a new idea and by using intelligent optimization methods, the non-linear differential equations governing viscoelastic nanofluids for the Sakiadis flow and heat transfer problem can be solved. The method combines the neural network and intelligent optimization algorithms and resolves the shortcomings of the previous methods. The present method can be utilized for solving high-order boundary value problems and nonlinear differential equations and there is no need for small parameters, linearization or convergence parameter control. Regarding the optimized structure of the trial solution used in this method, the solution is

convergent. In addition, this method is very powerful, yet simple to solve differential equations. The aim of the present study is to solve the viscoelastic nanofluids ill- posed equations using the combined method of neural network and intelligent optimization (Fig. 1).

2. Artificial neural networks

The main idea of the neural networks is inspired by the way the biological nervous system performs. In fact, it can be stated that the neural network is a form of artificial intelligence that mimics the learning process of a human brain. The system consists of a large number of inter-connected processing elements called neurons, that each neuron performs a simple command [45].

A data structure can be designed by the help of a programming knowledge that simulates the operation of a neuron. Then, an intended network is learnt by forming a network of inter-connected artificial neurons and using a learning algorithm. This structure was introduced in 1962 CE by Rosenblatt [52], showing a high performance in estimation and approximation of functions [53].

In multi-layer neural networks, the input layer receives data, and there are many hidden layers, that receive data from the previous layers, and finally, the output layer which shows the result of the calculations. Fig. 2 shows an example of a multi-layer neural network.

One of the major factors in neural network is the network topology. One of the simplest and yet most efficient arrangements of the neural network is the Multi-Layer Perceptron or MLP which is a part of forward networks and is formed of an input layer, one or more hidden layers and an output layer. In this structure, all the neurons in one layer are connected to all neurons in the next layer [45]. In order to increase the number of layers of a perceptron, the number of its hidden layers should be increased. A multi-layer perceptron model is shown in Fig. 3.

The most important application of multi-layer neural networks is their ability to approximate the functions. According to Kolmogorov existence theorem [54], each continuous function of n variables can be approximated by a three-layer perceptron with $n \times (2n + 1)$ nodes. Thus, it can be stated that the accuracy of functions approximation do not depend on the number of the network hidden layers, but it depends entirely on the number of hidden layer neurons. Fig. 4 shows the neural network with three layers (input layer, hidden layer and output layer) with one input (x), one hidden layer with H neuron and one output N (x, p). In a perceptron, the output is $N = \sum_{i=1}^{H} v_i s(z_i)$ where $z_i = w_i x + b_i$ and wi, bi and vi are weight parameters of the neural network and s is an arbitrary sigmoid function.

In this study, the multi-layer perceptron is used for forming a model of (a function of many variables) of input data. Here, a neural network training minimizes the error function. Thus, the neural network is allowed to use the theory of differential equations to form a function including neural network adjustable variables [51]. By minimizing this function, optimized adjustable variables are obtained for the desired multi-layer perceptron. The analytic function can be used to compute the solution of a differential equation.

3. Particles Swarm optimization algorithm (PSO)

The Particles Swarm Optimization method which acts based on a collective search and is simulated based on social behavior of a group of birds, is presented by Eberhart and Kennedy [46]. In this method, a group of particles searches collectively in the domain of the possible solutions, and during the search, the particles exchange local information with other particles. Naturally, this collective search can result in a better solution than an individual search.

In fact, in general, it can be said that the PSO method is a method of global minimization that can be used to face problems, which have a point or level in n-dimensional space of the solution. In this method, a group of particles is formed and an initial velocity is assigned to each of them. Also, communication channels are considered between the particles. Then, these particles move in the solution domain. Over time, the particles are accelerated toward the particles having values that are more favorable.

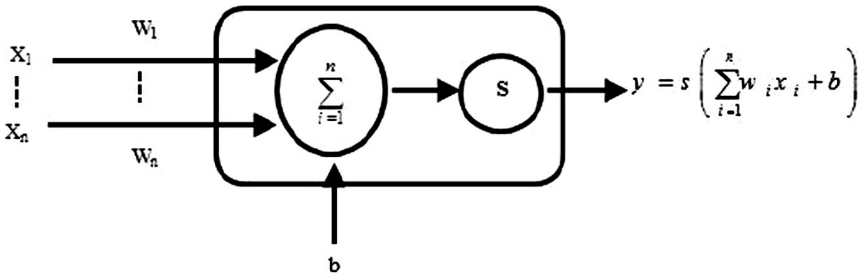

Fig. 1. An artificial neural network (perceptron).

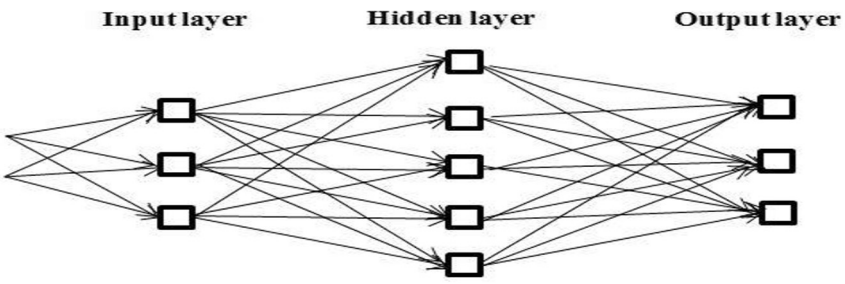

Fig. 2. Multi-layered neural networks.

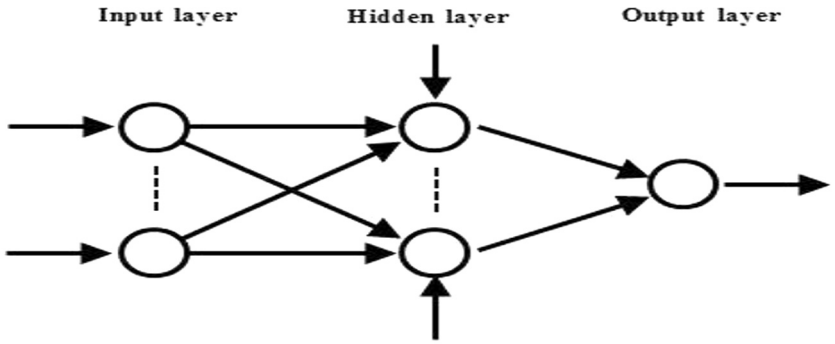

Fig. 3. A multi-layered perceptron.

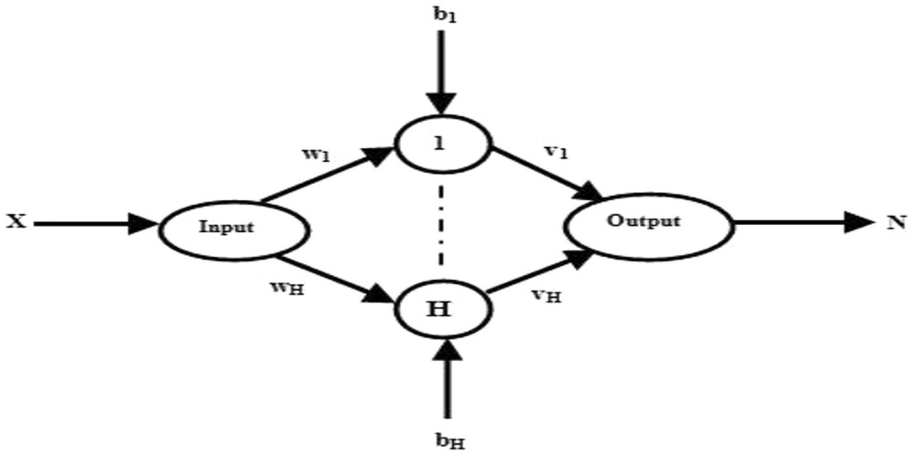

Fig. 4. A three-layered neural network.

In the PSO method, each particle has a position and a velocity, and the motion of the particle is adjusted in the search space according to personal information (the best position the particle has achieved so far) and social information (the best position obtained by other particles). In the PSO method, each particle i has a position Z_i and velocity v_i which is updated in in each search step:

$$\vec{v}_i = \omega\,\vec{v}_i + c_1 r_{1i}\left(\vec{\rho}_i - \vec{Z}_i\right) + c_2 r_{2i}\left(\vec{\rho}_g - \vec{Z}_i\right) \tag{1}$$

where ω is weight coefficient, $\vec{\rho}_i$ is the best position the particle has achieved so far, $\vec{\rho}_g$ is the best position in the overall population, r_1 and r_2 are random numbers between [0–1] which cause solution method get out of definite method, c_1 and c_2 are constant positive coefficients called acceleration coefficients that determine the share of personal information and social information relates parts. The position of each particle at each step is updated by adding the velocity vector to the position vector:

$$\vec{Z}_i = \vec{Z}_i + \vec{v}_i \tag{2}$$

Among the important parameters in the PSO algorithm, it can be referred to the weight coefficient ω, the maximum number of iteration (t) and the initial population (n). More details about the swarm optimization method can be found in [55,56].

4. Mathematical formulation

In most cases, the basic equations of viscoelastic fluids are so complex that they cannot be used in a theoretical analysis. Among the variety of models available, the second-order fluid model can be considered as of the most interest. One of the important features of the second-order fluid is that its viscosity is constant as a Newtonian fluid, and thus some of un-necessary complex effects can be neglected [10]. The fundamental equation of an incompressible viscoelastic fluid of second-order in the most general case can be written as follows [13]:

$$\tau = -pI + \mu A_1 + \alpha_1 A_2 + \alpha_2 A_1^2 \tag{3}$$

In the above equation, τ is the stress tensor, I is the unit tensor, μ is the viscosity, α_1 and α_2 are stress coefficients and A is the kinematics stress tensor and is obtained from the following equation [10]:

$$\begin{aligned} A_1 &= grad\ \boldsymbol{V} + (grad\ \boldsymbol{V})^T \\ A_2 &= \tfrac{dA_1}{dt} + (grad\ \boldsymbol{V})^T A_1 + A_1 (grad\ \boldsymbol{V}) \end{aligned} \tag{4}$$

In the above equation, V is velocity and d/dt is the material derivative. Experiments show that the following relations are applicable for second-order fluids [10]:

$$\mu \geqslant 0, \quad \alpha_1 \leqslant 0, \quad \alpha_1 + \alpha_2 \neq 0 \tag{5}$$

Considering Eqs. (4) and (5), the stress components in steady conditions are [13]:

$$\tau_{ij} = 2\mu_0 d_{ij} - 2K_0\left(\frac{Dd_{ij}}{Dt} - \frac{\partial v_j}{\partial x_m} d_{im} - \frac{\partial v_i}{\partial x_m} d_{mj}\right) \tag{6}$$

where d_{ij} can be obtained as follows:

$$d_{ij} = \frac{1}{2}\left[\frac{\partial V_i}{\partial x_j} + \frac{\partial V_j}{\partial x_i}\right] \tag{7}$$

Hence, the following equation is presented for the shear stress of the viscoelastic nanofluid over a moving flat plate [13]:

$$\tau_{xy} = \mu_0 \frac{\partial u}{\partial y} - K_0 \left[u \frac{\partial^2 u}{\partial x \partial y} + v \frac{\partial^2 u}{\partial y^2} + v \frac{\partial u}{\partial x} \frac{\partial u}{\partial y} \right] \tag{8}$$

The two-dimensional, steady, incompressible and quiescent flow of a viscoelastic nanofluid is considered over a hot flat plate. In Sakiadis flow, it is assumed that the fluid is static and the flat plate is moving at a constant velocity of U in parallel with the plate. The x-axis is along the plate and the y-axis is perpendicular to it. It is assumed that the plate is held at the constant temperature and concentration of T_w and C_w, respectively. Far from the plate where the fluid is quiescent, the temperature and concentration of the nanofluid are the ambient temperature (T_∞) and concentration (C_∞) of the viscoelastic nanofluid. In addition, it is assumed that the nanoparticles and the viscoelastic fluid are in local thermal equilibrium. It is assumed that the temperature difference is limited and hence, the thermodynamic properties of the nanofluids are constant and the pressure gradient and the external forces are assumed to be negligible. Following the Buongiorno model, the two mechanisms of Brownian motion and thermophoresis are taken into account for the heat transfer of a nanofluid. Given the above assumptions, the governing equations are as follows [18,44,57]:

$$\begin{aligned}
&\tfrac{\partial u}{\partial x} + \tfrac{\partial v}{\partial y} = 0 \\
&u \tfrac{\partial u}{\partial x} + v \tfrac{\partial u}{\partial y} = U_\infty \tfrac{dU_\infty}{dx} + \nu \left(\tfrac{\partial^2 u}{\partial y^2} \right) - \tfrac{k_0}{\rho} \left[u \tfrac{\partial^3 u}{\partial x \partial y^2} + v \tfrac{\partial^3 u}{\partial y^3} + \tfrac{\partial u}{\partial x} \tfrac{\partial^2 u}{\partial y^2} - \tfrac{\partial u}{\partial y} \tfrac{\partial^2 u}{\partial x \partial y} \right] \\
&u \tfrac{\partial T}{\partial x} + v \tfrac{\partial T}{\partial y} = \alpha_m \nabla^2 T + \left(\tfrac{(\rho C)_p}{(\rho c)_f} \right) \left[D_B \tfrac{\partial C}{\partial y} \tfrac{\partial T}{\partial y} + \tfrac{D_T}{T_\infty} \left(\tfrac{\partial T}{\partial y} \right)^2 \right] \\
&u \tfrac{\partial C}{\partial x} + v \tfrac{\partial C}{\partial y} = D_B \tfrac{\partial^2 C}{\partial y^2} + \tfrac{D_T}{T_\infty} \tfrac{\partial^2 T}{\partial y^2}
\end{aligned} \tag{9}$$

subject to the following boundary conditions:

$$\begin{aligned}
&@y = 0 : u = U, \quad v = 0, \quad T = T_w, \quad C = C_w \\
&@y = \infty : u = 0, \quad v = 0, \quad T = T_\infty, \quad C = C_\infty
\end{aligned} \tag{10}$$

where in these equations, u and v are the velocity components along the x, y directions; ν is the kinematic viscosity, k_0 is the viscoelastic parameter (Weissenburg number), ρ_f is the basic fluid density, ρ_p is the density of nanoparticles, α is the thermal diffusion coefficient, C is the concentration of nanoparticles and D_B and D_T are the Brownian and thermophoresis diffusion coefficients, respectively. In order to transform the governing partial differential equations into a set of ordinary differential equations, the following similarity variables are introduced [44]:

$$\begin{aligned}
&u = U_\infty f'(\eta), \quad V(\eta) = \frac{U_\infty}{2\sqrt{Re_x}} (\eta f' - f), \\
&\eta(x,y) = \sqrt{\frac{U_\infty}{\nu x}} y, \quad \theta(\eta) = \frac{T - T_\infty}{T_w - T_\infty}, \quad \phi(\eta) = \frac{C - C_\infty}{C_w - C_\infty}
\end{aligned} \tag{11}$$

In the above equation, η is the similarity variable. Invoking Eqs. (6), (7) and (11), the governing equations are achieved as follows:

$$\begin{aligned}
&f''' + \frac{1}{2} f' f'' + \frac{K}{2} \left(f f^{iv} + 2 f' f''' - f''^2 \right) = 0 \\
&\frac{1}{Pr} \theta'' + f \theta' + Nb \theta' \phi' + Nt \theta'^2 = 0 \\
&\phi'' + Lef \phi' + \frac{Nt}{Nb} \theta'' = 0
\end{aligned} \tag{12}$$

Subject to the following transformed boundary conditions:

$$\begin{aligned}
&f = 0, f' = 1, \quad \theta = 1, \quad \phi = 1 : \eta = 0 \\
&f' = 0, \quad \theta = 0, \quad \phi = 0 : \eta \to \infty
\end{aligned} \tag{13}$$

where the prime represents an ordinary derivative with respect to η and the non-dimensional parameters are as follows:

$$\begin{aligned}
&Pr = \frac{\upsilon}{\alpha_m}, \quad Le = \frac{\upsilon}{D_B}, \quad Nb = \frac{(\rho C)_p D_B (C_w - C_\infty)}{(\rho C)_f \upsilon}, \\
&Nt = \frac{(\rho C)_p D_T (T_w - T_\infty)}{(\rho C)_f T_\infty \upsilon}
\end{aligned} \tag{14}$$

where Pr, Le, Nb and Nt respectively denote the Prantl number, Lewis number, Brownian motion parameter and the thermophoresis parameter. The shear stress at the wall as well as the Nusselt number and the Sherwood number are significant parameters of interest for flow, heat and mass transfer of nanofluids which are introduced as [57]:

$$Nu = \frac{x q_w}{k(T_w - T_\infty)}, \quad Sh = \frac{x q_m}{D_B (T_w - T_\infty)} \tag{15}$$

where q_w and q_m are the wall heat and mass fluxes, respectively. Using the similarity variables in Eq. (11), the following equations are obtained:

$$\begin{aligned}
\tau_{xy}\big|_{y=0} &= (1 - K) \mu_0 U_\infty \sqrt{\frac{U_\infty}{\nu x}} f''(0), \quad Re_x^{-\frac{1}{2}} Nu_x \\
&= -\theta'(0), \quad Re_x^{-\frac{1}{2}} Sh_x = -\phi'(0)
\end{aligned} \tag{16}$$

It is noteworthy that Kuznetsov and Nield [57] referred to $Re_x^{-1/2} Nu_x$ and $Re_x^{-1/2} Sh_x$ as the reduced Nusselt number ($Nur = -\theta'(0)$) and the reduced Sherwood number ($Shr = -\phi'(0)$), respectively.

5. Solution method

Consider the transformed form of the governing equations of a second-order fluid in Sakiadis flow, heat and mass transfer, expressed by Eq. (12) subject to Eq. (13). To solve these equations, the domain of the solution (D) is discretized with $m = 61$ points with equal distance. In this case, the governing equations at each point can be written as:

$$\begin{aligned}
&f'''(\eta_i) + \frac{1}{2} f(\eta_i) f''(\eta_i) + \frac{K}{2} \left(f(\eta_i) f^{iv}(\eta_i) + 2 f'(\eta_i) f'''(\eta_i) - f''^2(\eta_i) \right) = 0 \\
&\frac{1}{Pr} \theta''(\eta_i) + f(\eta_i) \theta'(\eta_i) + Nb \theta'(\eta_i) \phi'(\eta_i) + Nt \theta'^2(\eta_i) = 0 \\
&\phi''(\eta_i) + Lef(\eta_i) \phi'(\eta_i) + \frac{Nt}{Nb} \theta''(\eta_i) = 0
\end{aligned} \tag{17}$$

where the boundary conditions are provided in Eq. (13). $y_T\left(\eta, \vec{P_1}\right)$, $\theta_T\left(\eta, \vec{P_2}\right)$ and $\phi_T\left(\eta, \vec{P_3}\right)$ are approximate solutions of the above equations, where the a subscript T denotes the trial function and P_1, P_2 and P_3 are adjustable parameters involving weights and biases of three-layered feed-forward neural networks (as shown in Fig. 4). For each of the above equations, a trial function can be considered. Thus, the error equation is obtained for each of the equations as follows:

$$\begin{aligned}
E_1(\vec{P}) = \sum_{i=1}^{m} \Bigg[&\frac{d^3 y_T\left(\eta_i, \vec{P_1}\right)}{d\eta^3} + \frac{1}{2} y_T\left(\eta_i, \vec{P_1}\right) \frac{d^2 y_T\left(\eta_i, \vec{P_1}\right)}{d\eta^2} \\
&+ \frac{K}{2} \Bigg(y_T\left(\eta_i, \vec{P_1}\right) \frac{d^4 y_T\left(\eta_i, \vec{P_1}\right)}{d\eta^4} + 2 \frac{dy_T\left(\eta_i, \vec{P_1}\right)}{d\eta} \frac{d^3 y_T\left(\eta_i, \vec{P_1}\right)}{d\eta^3} \\
&- \left(\frac{d^2 y_T\left(\eta_i, \vec{P_1}\right)}{d\eta^2} \right)^2 \Bigg) \Bigg] = 0
\end{aligned}$$

$$E_2(\vec{P}) = \sum_{i=1}^{m}\left[\frac{1}{Pr}\frac{d^2\theta_T\left(\eta_i,\vec{P_2}\right)}{d\eta^2}+\frac{1}{2}y_T\left(\eta_i,\vec{P_1}\right)\frac{d\theta_T\left(\eta_i,\vec{P_2}\right)}{d\eta} + Nb\frac{d\theta_T\left(\eta_i,\vec{P_2}\right)}{d\eta}\frac{d\phi_T\left(\eta_i,\vec{P_3}\right)}{d\eta}+Nt\left(\frac{d\theta_T(\eta_i,\vec{P_2})}{d\eta}\right)^2\right]=0$$

$$E_3(\vec{P}) = \sum_{i=1}^{m}\frac{d^2\phi_T\left(\eta_i,\vec{P_3}\right)}{d\eta^2}+\frac{Le}{2}y_T\left(\eta_i,\vec{P_1}\right)\frac{d\phi_T\left(\eta_i,\vec{P_3}\right)}{d\eta} + \frac{Nt}{Nb}\frac{d^2\theta_T\left(\eta_i,\vec{P_2}\right)}{d\eta^2}=0 \quad (18)$$

where the boundary conditions should also be satisfied. In order to convert the equation to an unconstrained optimization problem, each of the trial solutions is considered as the sum of the two parts. The first part satisfies the initial/boundary conditions. The second part of the solution includes adjustable parameters of the neural network that are obtained by the optimization method. In order to calculate the error function, trial solution derivatives to η are required. Among the various transfer functions that are used in neural networks, Sigmoid function $s = (1/1 + \exp(-\eta))$ is used in this study. Considering the boundary conditions in the Sakiadis problem, i.e. Eq. (13), the trial solutions for flow, heat and mass transfer are considered as follows:

$$y_T = a_0\eta^3 - \left(\frac{1+3a_0b^2}{2b}\right)\eta^2+\eta+\eta^2(\eta-b)^2N\left(\eta,\vec{p_1}\right)$$

$$\theta_T = a_1\eta^3+a_2\eta^2-\left(\frac{1+a_1b^3+a_2b^2}{b}\right)\eta+1+\eta(\eta-b)N\left(\eta,\vec{p_2}\right)$$

$$\phi_T=\theta_T=a_3\eta^3+a_4\eta^2-\left(\frac{1+a_3b^3+a_4b^2}{b}\right)\eta+1+\eta(\eta-b)N(\eta,\vec{p_3}) \quad (19)$$

In Eq. (19), a_0 is the adjustable parameter of the trial solution of the flow function, a_1 and a_2 are adjustable parameters of the trial solution of the temperature function and a_3 and a_4 are adjustable parameters of the trial solution of the concentration function and are determined by the help of the optimization method. $N\left(\eta,\vec{P_1}\right)$, $N\left(\eta,\vec{P_2}\right)$ and $N\left(\eta,\vec{P_3}\right)$ are three-layer perceptron neural networks that includes adjustable parameters of the neural network. The above equation satisfies all problem boundary conditions in a Sakiadis flow (i.e. Eq. (13)). Now, Eq. (18) shows an unconstraint optimization problem in which y_T, θ_T and ϕ_T, satisfying the boundary conditions, are introduced in Eq. (19). Now, an optimization method is required to find the optimum values of a_0 to a_4 as well as the network parameters $\vec{P_1}$ to $\vec{P_3}$ regarding to the objective function of Eq. (18).

6. Results and discussion

The optimizations algorithm and the objective function of Eq. (18) are coded in MATLAB 2009. The physical value of infinity (η_∞) is denoted by b and is assumed large enough to satisfy the asymptotic boundary conditions (i.e. $b = 6$). Five neurons ($H = 5$) for each trial function (i.e. y_T, θ_T and ϕ_T) are considered, and the objective functions were evaluated as the sum of the error in 61 uniform points in the domain of the solution ($m = 61$). The following default parameters [56] were found suitable for the PSO by experiment:

The initial population = 150, weighted coefficient = 0.9, the acceleration factor = 2.5, the maximum number of iteration = 150.

The governing equations (Eq. (12)) were solved for the following combination of the non-dimensional parameters $K = 0.2$, $Le = Pr = 10$ and $Nt = Nb = 0.1$ by optimizing Eq. (18) using the PSO method. The adjustable parameters of the first part of the flow function trial solution (i.e. a_0 to a_4) are obtained as $a_0 = 0.0137$, $a_1 = 0.0356$, $a_2 = 0.4316$, $a_3 = 0.0127$ and $a_4 = 0.2755$. The network parameters for $\vec{P_1}$ are also obtained and summarized in Table 1. In this case, the values of the error for the trial functions are equal to $E_1\left(\vec{P_1}\right) = 5.55\times10^{-3}$, $E_2\left(\vec{P_1}\right) = 3.84\times10^{-2}$ and $E_3\left(\vec{P_1}\right) = 1.84\times10^{-2}$.

Considering the value of a_0 and the network parameters in Table 1, the obtained solution, representing the flow of the viscoelastic nanofluid, is summarized as follow:

$$y_T(\eta,\vec{p_1}) = 0.0137\eta^3-0.2066\eta^2+\eta+\eta^2(\eta-6)^2 \times\left(\frac{0.1522}{1+e^{0.2409\eta+9.7814}}+\frac{-0.3730}{1+e^{-0.6364\eta-1.9691}}+\frac{-0.0558}{1+e^{0.0110\eta+1.1142}} +\frac{0.3859}{1+e^{-0.6351\eta-2.0410}}+\frac{-0.0031}{1+e^{-0.0200\eta+1.8320}}\right) \quad (20)$$

The temperature and concentration equations are also solved using HNNPSO where the obtained functions can be summarized as follows:

$$\theta_T(\eta,\vec{p_2}) = 0.0356\eta^3+0.3416\eta^2-4.0378\eta+1+\eta(\eta-6) \times\left(\frac{0.6078}{1+e^{1.8636\eta-2.1330}}+\frac{-1.3411}{1+e^{0.1418\eta+0.0070}}+\frac{0.4939}{1+e^{2.6321\eta-0.4734}} +\frac{1.0210}{1+e^{-1.7557\eta+1.5879}}+\frac{0.2102}{1+e^{-1.4388\eta-3.8562}}\right) \quad (21)$$

$$\phi_T\left(\eta,\vec{p_3}\right) = 0.0127\eta^3+0.2755\eta^2-2.2768\eta+1+\eta(\eta-6) \times\left(\frac{0.0547}{1+e^{-2.6320\eta+3.9761}}+\frac{-0.6146}{1+e^{-0.1793\eta+0.7671}}+\frac{0.2344}{1+e^{0.9597\eta-3.8594}} +\frac{0.1274}{1+e^{-4.8882\eta+1.3620}}+\frac{0.6763}{1+e^{-0.6325\eta+2.3988}}\right) \quad (22)$$

The results of the viscoelastic fluid Sakiadis flow solution using the neural network-intelligent optimization method for three, four and five neurons are shown in Table 2. As it can be seen, by increasing the number of neurons in the hidden layer of the neural network from three neurons to five neurons, better results are obtained. According to the survey, increasing the number of neurons to more than five neurons does not cause much change in the accuracy of the solution obtained.

Table 3 shows a comparison between the results of the Homotopy analysis method [12], forth-order predictor-corrector finite-difference method [13] and the neural network-intelligent optimization method (with 5 neurons in the present study) for

Table 1
Obtained optimal adjustable parameters in trial function $y_T(\eta,\vec{P}_1)$ when $Le = Pr = 10$, $Nb = Nt = 0.1$ and $K = 0.2$.

Index (i)	Adjustable parameters in ANN		
	w_i	b_i	v_i
1	−0.2409	−9.7814	0.1522
2	0.6364	1.9691	−0.3730
3	−0.0110	−1.1142	−0.0558
4	0.6351	2.0410	0.3859
5	0.0200	−0.8320	−0.0021

Table 2
Comparison between results obtained via HNNPSO method for 3 neurons, 4 neurons and 5 neurons.

Weissenberg number (K)	$-f''(0)$			
	Fourth-order predictor-corrector method [13]	HNNPSO		
		3 neurons	4 neurons	5 neurons
0.0	0.44349	0.45031	0.44695	0.44255
0.4	0.45658	0.44404	0.45466	0.45871
0.8	0.47529	0.47135	0.47173	0.47493
1.2	0.50525	0.48912	0.48378	0.49169

Table 3
Comparison between results obtained via HNNPSO method (5 nonrons), fourth-order predictor-corrector method and HAM for different Weissenberg number (K).

Weissenberg number (K)	$-f''(0)$			
	Fourth-order predictor-corrector method [13]	HAM [12]	HNNPSO	% Error = $\left\|\frac{f(\eta)_{NM}-f(\eta)_{HNNPSO}}{f(\eta)_{NM}}\right\| \times 100$
0.0	0.44349	–	0.44255	0.21
0.2	–	0.44975	0.45294	0.71
0.4	0.45658	0.45681	0.45871	0.46
0.5930	–	0.46491	0.46501	0.01
0.75	–	0.47261	0.47082	0.38
0.8	0.47529	–	0.7493	0.01
0.85	–	0.47820	0.47721	0.21
0.95	–	0.48445	0.47929	1.06
1.2	0.50525	–	0.49169	2.6

Table 4
Variation of *Nur* and *Shr* as a function of Weissenberg number (K) for $Pr = Le = 10$ and $Nb = Nt = 10$.

Weissenberg number (K)	*Nur*	*Shr*
0.0	0.6904	1.5704
0.2	0.6881	1.5699
0.4	0.6668	1.6622
0.6	0.6895	1.5645

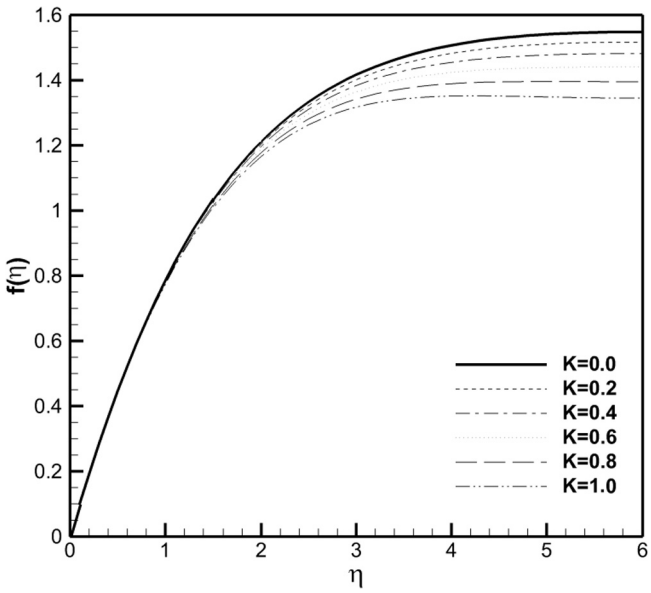

Fig. 5. Effect of various Weissenberg number on $f(\eta)$.

the case of a pure fluid for different values of the Weissenberg number. The results of this table indicate the accuracy of the present solution using HNNPSO.

It is worth noticing that the error in Table 3 is measured by comparison with the results of the fourth-order predictor-corrector finite-difference method reported by Tonekaboni et al.

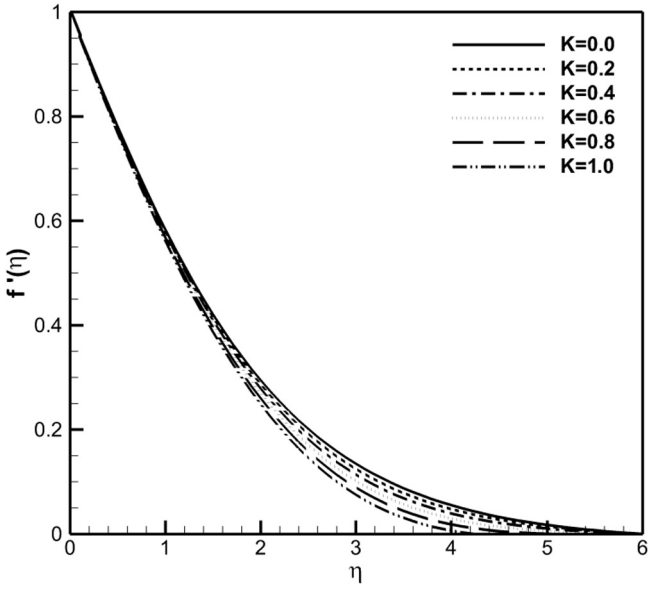

Fig. 6. Effect of various Weissenberg number on $f'(\eta)$.

[13]. However, in some cases in which the values of $f''(0)$ were not reported by Tonekaboni et al. [13] the values $f''(0)$ evaluated using the HAM and reported by Munawar et al. [12] were utilized to estimate error in Table 3. In the evaluation of the error in Table 3, the subscripts of *NM* and *HNNPSO* indicate the numerical solution (reported by Tonekaboni et al. [13]) and the results of the present study, respectively. As seen, the results of Table 3 show good agreement between the results of the present study and those reported by previous researchers. It is worth noticing that using the present method would also results in analytical expressions for flow, heat and mass transfer. According to the results presented in Table 3, it is clear that by increasing the fluid elasticity (K), the value of $f''(0)$ slightly increases, and thus, according to Eq. (16), the value of the wall shear stress decreases. This is because of the fact that the wall shear stress is a decreasing function of K

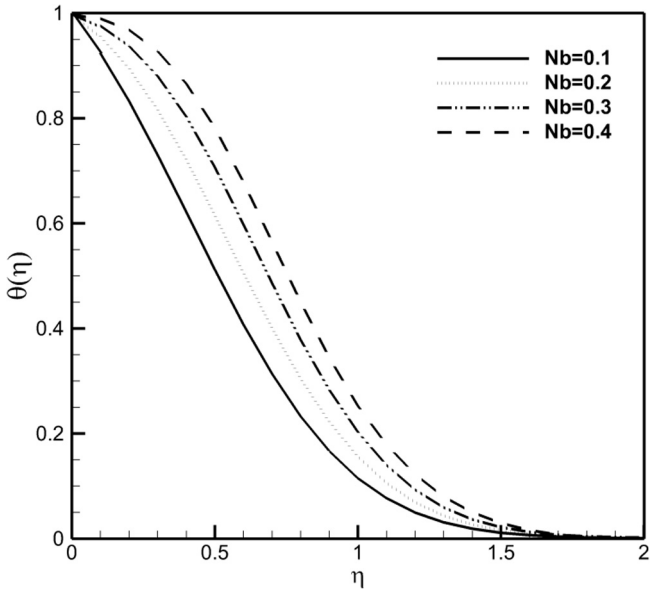

Fig. 7. Effect of various *Nb* on $\theta(\eta)$ when $K = 0.5930$, $Le = Pr = 10$ and $Nt = 0.1$.

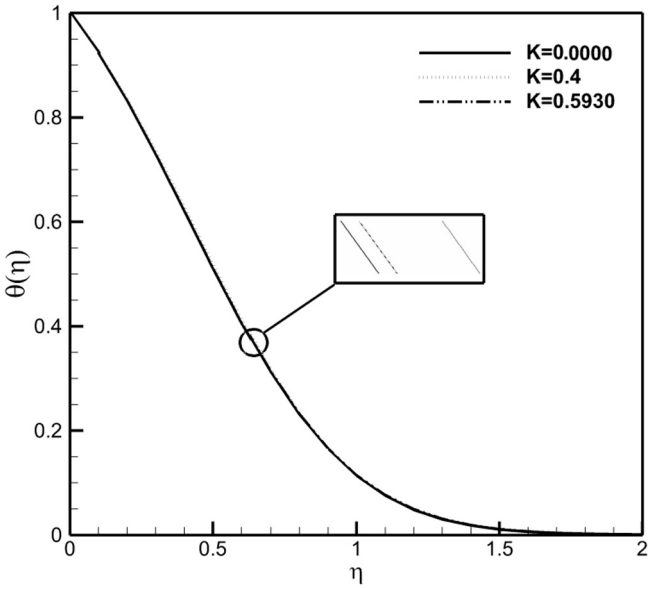

Fig. 9. Effect of various Weissenberg number on $\theta(\eta)$ when $Le = Pr = 10$ and $Nb = Nt = 0.1$.

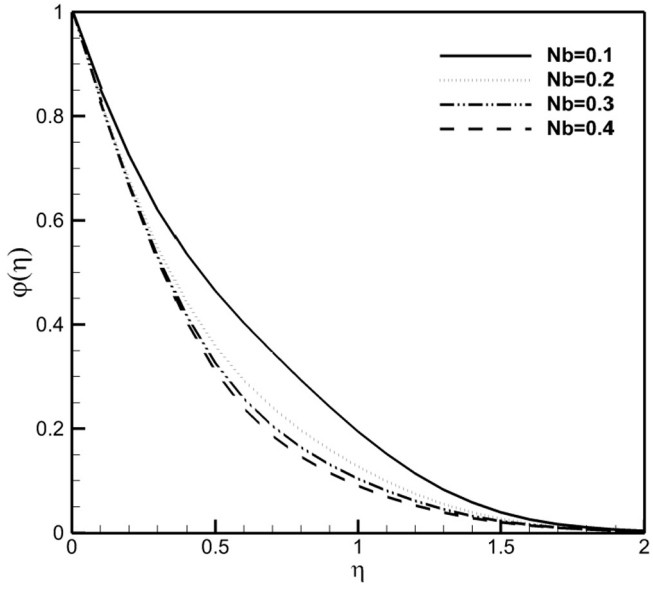

Fig. 8. Effect of various *Nb* on $\varphi(\eta)$ when $K = 0.5930$, $Le = Pr = 10$ and $Nt = 0.1$.

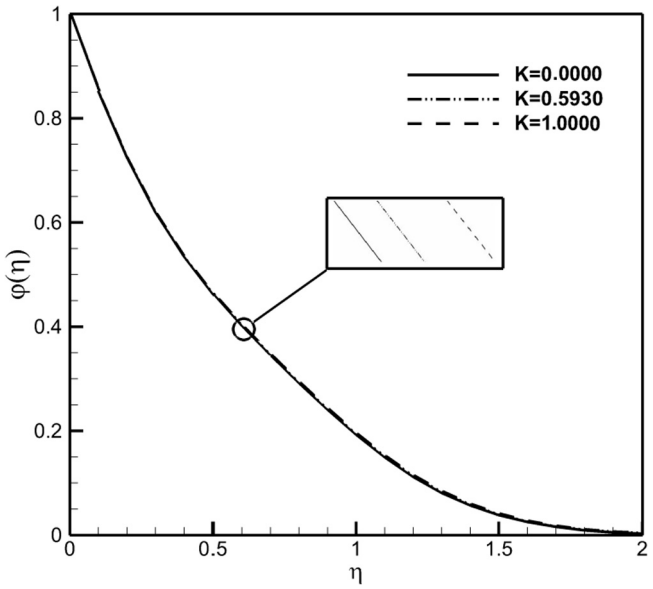

Fig. 10. Effect of various Weissenberg number on $\varphi(\eta)$ when $Le = Pr = 10$ and $Nb = Nt = 0.1$.

and an increasing function of $f''(0)$. This result has an important industrial application where less force is needed to pull a moving belt in a viscoelastic fluid by increasing the fluid elasticity, which increases the speed of production.

The values of the reduced Nusselt number and the reduced Sherwood number are presented in Table 4 for the case of a viscoelastic nanofluid when $Pr = Le = 10$ and $Nb = Nt = 10$. The results show that the reduced Nusselt number is almost a decreasing function of the fluid elasticity (Weissenberg number) when the values of the fluid elasticity are small ($K \leq 0.4$). The effect of different non-dimensional parameters on the non-dimensional stream function, flow velocity, temperature and concentration of a viscoelastic nanofluid are plotted in the Figs. 5–9. Figs. 5 and 6 depict the stream function and the velocity profiles (f) and (f') for different values of the Weissenberg number.

As seen in Figs. 5 and 6, it is clear that the increase of the fluid elasticity (K) decreases the boundary layer thickness. In other words, by increasing the Weissenberg number, the fluid's normal stresses tend to accelerate the fluid near the plate, but they would decrease the penetration of the fluid motion into the quiescent part of the ambient fluid. Figs. 7 and 8 show respectively profiles for the non-dimensional temperature distribution and concentration of a viscoelastic nanofluid for selected values of the Brownian motion parameter. As it can be seen, by increasing the Brownian motion parameter, the fluid temperature and the nanoparticles concentration are decreased. Fig. 7 depicts that the decrease of the Brownian motion parameter significantly increases the slope of the temperature profiles at the surface, and hence, it results in augmentation of heat transfer from the surface.

Figs. 9 and 10 present the dimensionless temperature distribution and nanoparticles concentration of a viscoelastic nanofluid for selected values of the Weissenburg numbers, respectively. These figures indicate that the effect of variation of the Weissenberg

number (fluid elasticity change) on the boundary layer thickness is not significant. This is because of the fact that the variation of the Weissenberg number smoothly changes the velocity profiles, and consequently, the variation of the velocity profiles affects the temperature and concentration profiles. Hence, the effect of variation of the Weissenberg number on the temperature and concentration profiles is almost negligible.

7. Conclusion

The problem of boundary layer flow and heat and mass transfer of viscoelastic nanofluids for the Sakadis problem was analyzed. A similarity solution approach was utilized to transform the governing partial differential equations into a set of non-linear high-order ordinary differential equations. A new method using the artificial neural network and the intelligent optimization algorithm (HNNPSO) was utilized to obtain the solution expressions for the boundary layer profiles. The solution results were compared with the results of the fourth-order predictor-corrector finite-difference method and the Homotopy analysis method for the case of a regular fluid. The results indicated the robustness and the accuracy of the present method. It was found that using a very few number of neurons could provide acceptable accuracy. The solution results for flow, heat and mass transfer of viscoelastic nanofluids indicated that by increasing the fluid elasticity, the value of $f''(0)$ was increased, and the value of the wall shear stress was decreased. However, the variation of the Weissenberg number (K) did not show a significant effect on the thermal and concentration boundary layer thicknesses. The decrease of the Brownian motion parameter boosted the heat transfer from the plate.

References

[1] H.A. Barnes, A Handbook of Elementary Rheology, University of Wales Institute of Non-Newtonian Fluid Mechanics, 2000.
[2] L. Zhang, Y. Ding, M. Povey, D. York, ZnO nanofluids – a potential antibacterial agent, Prog. Nat. Sci. 18 (2008) 939–944.
[3] K. Hirota, M. Sugimoto, M. Kato, K. Tsukagoshi, T. Tanigawa, H. Sugimoto, Preparation of zinc oxide ceramics with a sustainable antibacterial activity under dark conditions, Ceram. Int. 36 (2008) 497–506.
[4] H. Tyagi, Radiative and Combustion Properties of Nanoparticle-Laden Liquids, Arizona State University, 2008.
[5] H. Tyagi, P. Phelan, R. Prasher, Predicted efficiency of a low-temperatur nanofluid-based direct absorption solar collector, J. Solar Energy Eng. 131 (2009) 041004.
[6] R.P. Chhabra, J.F. Richardson, Non-Newtonian Flow in the Process Industries, Butterworth-Heinemann, Oxford, 1999.
[7] J. Kevorkian, J.D. Cole, Perturbation Methods in Applied Mathematics, Springer-Verlag, New York, 1981.
[8] S. Liao, Proposed Homotopy Analysis Techniques for the Solution of Nonlinear Problems, Shanghai Jiao Tong University, 1992.
[9] G. Adomian, Solving Frontier Problems of Physics: The decomposition method, Kluwer Academic Publishers, 1994.
[10] K. Sadeghy, M. Sharifi, Local similarity solution for the flow of a "second-grade" viscoelastic fluid above a moving plate, Int. J. Non-Linear Mech. 39 (2004) 1265–1273.
[11] R. Cortell, Analysing flow and heat transfer of a viscoelastic fluid over a semi-infinite horizontal moving flat plate, Int. J. Non-Linear Mech. 43 (2008) 772–778.
[12] S. Munawar, A. Mehmood, A. Ali, Comment on "Analysing flow and heat transfer of a viscoelastic fluid over a semi-infinite horizontal moving flat plate, IJNLM, 43 (2008) 772", Int. J. Non-Linear Mech. 46 (2011) 1280–1282.
[13] S.A. Madani Tonekaboni, R. Abkar, R. Khoeilar, On the study of viscoelastic Walters' B fluid in boundary layer flows, Math. Probl. Eng. (2012).
[14] H.M. Duwairi, R.A. Damseh, A.J. Chamkha, M.S. Abdel-Jaber, Transient convection flow of a viscoelastic fluid over a vertical surface, Appl. Math. Mech. 31 (2010) 557–564.
[15] G.K. Ramesh, A.J. Chamkha, B.J. Gireesha, MHD mixed convection viscoelastic fluid over an inclined surface with a non-uniform heat source/sink, Can. J. Phys. 91 (2013) 1074–1080.
[16] S.U.S. Choi, J.A. Eastman, Enhancing Thermal Conductivity of Fluids with Nanoparticles, American Society of Mechanical Engineers, New York, 1995.
[17] S.K. Das, S.U.S. Choi, W. Yu, T. Pradeep, Nanofluids, John Wiley & Sons, Inc., 2007, 389–397.
[18] J. Buongiorno, Convective transport in nanofluids, J. Heat Transf. 128 (2005) 240–250.
[19] T. Hayat, A. Aziz, T. Muhammad, A. Alsaedi, On magnetohydrodynamic three-dimensional flow of nanofluid over a convectively heated nonlinear stretching surface, Int. J. Heat Mass Transf. 100 (2016) 566–572.
[20] M. Mustafa, J. Ahmad Khan, T. Hayat, A. Alsaedi, Buoyancy effects on the MHD nanofluid flow past a vertical surface with chemical reaction and activation energy, Int. J. Heat Mass Transf. 108 (2017) 1340–1346.
[21] M.A. Sheremet, I. Pop, Natural convection in a wavy porous cavity with sinusoidal temperature distributions on both side walls filled with a nanofluid: Buongiorno's mathematical model, J. Heat Transf. 137 (2015) 072601.
[22] M.A. Sheremet, I. Pop, N. Bachokd, Effect of thermal dispersion on transient natural convection in a wavy-walled porous cavity filled with a nanofluid: Tiwari and Das' nanofluid model, Int. J. Heat Mass Transf. 92 (2016) 1053–1060.
[23] M. Sheikholeslami, T. Hayat, A. Alsaedi, MHD free convection of Al2O3–water nanofluid considering thermal radiation: a numerical study, Int. J. Heat Mass Transf. 96 (2016) 513–524.
[24] M.A. Sheremet, I. Pop, Mixed convection in a lid-driven square cavity filled by a nanofluid: Buongiorno's mathematical model, Appl. Math. Comput. 266 (2015) 792–808.
[25] T. Hayat, S. Qayyum, M. Imtiaz, A. Alsaedi, Comparative study of silver and copper water nanofluids with mixed convection and nonlinear thermal radiation, Int. J. Heat Mass Transf. 102 (2016) 723–732.
[26] T. Hayat, M. Javed, M. Imtiaz, A. Alsaedi, Convective flow of Jeffrey nanofluid due to two stretchable rotating disks, J. Mol. Liquids 240 (2017) 291–302.
[27] M. Imtiaz, T. Hayat, A. Alsaedi, Mixed convection flow of Casson nanofluid over a stretching cylinder with convective boundary conditions, Adv. Powder Technol. 27 (2016) 2245–2256.
[28] T. Hayat, S. Farooq, A. Alsaedi, B. Ahmad, Influence of variable viscosity and radial magnetic field on peristalsis of copper-water nanomaterial in a non-uniform porous medium, Int. J. Heat Mass Transf. 103 (2016) 1133–1143.
[29] T. Hayat, T. Muhammad, S.A. Shehzad, M.S. Alhuthali, J. Lu, Impact of magnetic field in three-dimensional flow of an Oldroyd-B nanofluid, J. Mol. Liquids 212 (2015) 272–282.
[30] T. Hayat, M. Ijaz Khan, M. Waqas, A. Alsaedi, Effectiveness of magnetic nanoparticles in radiative flow of Eyring-Powell fluid, J. Mol. Liquids 231 (2017) 126–133.
[31] T. Hayat, M. Waqas, S.A. Shehzad, A. Alsaedi, On model of Burgers fluid subject to magneto nanoparticles and convective conditions, J. Mol. Liquids 222 (2016) 181–187.
[32] T. Hayat, I. Ullah, T. Muhammad, A. Alsaedi, A revised model for stretched flow of third grade fluid subject to magneto nanoparticles and convective condition, J. Mol. Liquids 230 (2017) 608–615.
[33] T. Hayat, S. Qayyum, A. Alsaedi, A. Shafiq, Inclined magnetic field and heat source/sink aspects in flow of nanofluid with nonlinear thermal radiation, Int. J. Heat Mass Transf. 103 (2016) 99–107.
[34] T. Hayat, S. Qayyum, A. Alsaedi, S.A. Shehzad, Nonlinear thermal radiation aspects in stagnation point flow of tangent hyperbolic nanofluid with double diffusive convection, J. Mol. Liquids 223 (2016) 969–978.
[35] M. Imtiaz, T. Hayat, A. Alsaedi, Flow of magneto nanofluid by a radiative exponentially stretching surface with dissipation effect, Adv. Powder Technol. 27 (2016) 2214–2222.
[36] T. Hayat, M. Imtiaz, A. Alsaedi, Melting heat transfer in the MHD flow of Cu–water nanofluid with viscous dissipation and Joule heating, Adv. Powder Technol. 27 (2016) 1301–1308.
[37] T. Hayat, T. Muhammad, S.A. Shehzad, G.Q. Chen, I.A. Abbas, Interaction of magnetic field in flow of Maxwell nanofluid with convective effect, J. Magn. Magn. Mater. 389 (2015) 48–55.
[38] N.S. Bondareva, M.A. Sheremet, I. Pop, Magnetic field effect on the unsteady natural convection in a right-angle trapezoidal cavity filled with a nanofluid: Buongiorno's mathematical model, Int. J. Numer. Methods Heat Fluid Flow 25 (2015) 1924–1946.
[39] T. Hayat, S. Qayyum, M. Imtiaz, F. Alzahrani, A. Alsaedi, Partial slip effect in flow of magnetite-Fe_3O_4 nanoparticles between rotating stretchable disks, J. Magn Mag Mater 413 (2016) 39–48.
[40] F.M. Abbasi, T. Hayat, A. Alsaedi, Peristaltic transport of magneto-nanoparticles submerged in water: model for drug delivery system, Physica E 68 (2015) 123–132.
[41] T. Hayat, M. Imtiaz, A. Alsaedi, F. Alzahrani, Effects of homogeneous–heterogeneous reactions in flow of magnetite-Fe_3O_4 nanoparticles by a rotating disk, J. Mol. Liquids 216 (2016) 845–855.
[42] L.J. Sheu, H.S. Chiou, W.T. Weng, S.R. Lee, The onset of convection in a viscoelastic nanofluid layer, Electronic and Mechanical Engineering and Information Technology (EMEIT) (2011) 2044–2047.
[43] J.C. Yang, F.C. Li, W.W. Zhou, Y.R. He, B.C. Jiang, Experimental investigation on the thermal conductivity and shear viscosity of viscoelastic-fluid-based nanofluids, Int. J. Heat Mass Transf. 55 (2012) 3160–3166.
[44] M. Goyal, R. Bhargava, Boundary layer flow and heat transfer of viscoelastic nanofluids past a stretching sheet with partial slip conditions, Appl. Nanosci. 4 (2014) 761–767.
[45] D.J. Cavuto, An exploration and development of current artificial neural network theory and applications with emphasis on artificial life, A thesis submitted in partial fulfillment of the requirements for the degree of Master of Engineering, 1997.
[46] J. Kennedy, R. Eberhart, Particle swarm optimization, IEEE Int. Conf. Neural Netw. (1995) 1942–1948.

[47] D. Karaboga, B. Basturk, A powerful and efficient algorithm for numerical function optimization: Artificial Bee Colony (ABC) algorithm, J. Global Optim. 39 (2007) 459–471.
[48] H. Lee, I.S. Kang, Neural algorithm for solving differential equations, J. Comput. Phys. 91 (1990) 110–131.
[49] A.J. Meade Jr, A.A. Fernandez, The numerical solution of linear ordinary differential equations by feedforward neural networks, Math. Comput. Modell. 19 (1994) 1–25.
[50] I.E. Lagaris, A. Likas, D.I. Fotiadis, Artificial neural networks for solving ordinary and partial differential equations, IEEE Trans. Neural Netw. 9 (1998) 987–1000.
[51] A. Malek, R.S. Beidokhti, Numerical solution for high order differential equations using a hybrid neural network—optimization method, Appl. Math. Comput. 183 (2006) 260–271.
[52] S.P. Marvin Minsky, Perceptrons: An Introduction to Computational Geometry, M.I.T. Press, Cambridge, 1987.
[53] A. El-Bouri, S. Balakrishnan, N. Popplewell, Sequencing jobs on a single machine: a neural network approach, Eur. J. Oper. Res. 126 (2000) 474–490.
[54] K. Hornik, M. Stinchcombe, H. White, Multilayer feedforward networks are universal approximators, Neural Netw. 2 (1989) 359–366.
[55] I.C. Trelea, The particle swarm optimization algorithm: convergence analysis and parameter selection, Inf. Process. Lett. 85 (2003) 317–325.
[56] M. Jiang, Y.P. Luo, S.Y. Yang, Convergence analysis and parameter selection of the standard particle swarm optimization algorithm, Inf. Process. Lett. 102 (2007) 8–16.
[57] A.V. Kuznetsov, D.A. Nield, Natural convective boundary-layer flow of a nanofluid past a vertical plate, Int. J. Therm. Sci. 49 (2010) 243–247.